This document was prepared for the ETI by third parties under contract to the ETI. The ETI is making these documents and data available to the public to inform the debate on low carbon energy innovation and deployment.

Programme Area: Marine

Project: PerAWAT

Title: Development of a Computational Fluid Dynamics Mesoscale Tidal Channel Model

Abstract:

The aim of this deliverable is to demonstrate a working model of mesoscale tidal flows, and to provide a fully-validated approach for doing so, which can be utilised in WG3 WP2 D5b to model arrays of tidal turbines. In this report, the development, testing and validation of a mesoscale, three-dimensional tidal channel model is detailed. The modelling work used the computational fluid dynamics software Code Saturne, with unsteady Reynolds-averaged Navier-Stokes equations resolving the turbulent tidal flow. The simulations were large, fully parallel simulations, running on Eddie, the University of Edinburgh's parallel computing resource.

Context:

The Performance Assessment of Wave and Tidal Array Systems (PerAWaT) project, launched in October 2009 with £8m of ETI investment. The project delivered validated, commercial software tools capable of significantly reducing the levels of uncertainty associated with predicting the energy yield of major wave and tidal stream energy arrays. It also produced information that will help reduce commercial risk of future large scale wave and tidal array developments.

PerAWaT (MA 1003) report for WG3 WP2 D4

Development of a computational fluid dynamics mesoscale tidal channel model

Dr Angus Creech

University of Edinburgh

Final version
23 May 2013

Contents

1. Executive summary

The aim of this deliverable is to demonstrate a working model of mesoscale tidal flows, and to provide a fully-validated approach for doing so, which can be utilised in WG3 WP2 D5b to model arrays of tidal turbines.

In this report, the development, testing and validation of a mesoscale, three-dimensional tidal channel model is detailed. The modelling work used the computational fluid dynamics software *Code Saturne*, with unsteady Reynolds-averaged Navier-Stokes equations resolving the turbulent tidal flow. The simulations were large, fully parallel simulations, running on Eddie, the University of Edinburgh's parallel computing resource.

1.1 Approach

A real tidal channel was chosen as a template for constructing the model – the Sound of Islay between the islands of Islay and Jura, off the West Coast of Scotland. This is an appropriate choice, given that it is due to be used as a test bed for a demonstration tidal turbine array [1]. It possesses the qualities of a tidal site ideal for marine renewable energy generation.

Tests were conducted on the problem geometry, mesh resolution and turbulence profiles. These are detailed in section 4. The tests were mainly to address the often competing issues of accuracy versus computational resource, as more accurate simulations tend to require larger computers and more disc space. The results are used to determine an appropriate level of trade-off between the two.

Once this balance had been attained, simulations were run with the flow at different stages of a tidal cycle. An appraisal of the time-averaged downstream flow results was made to ensure that the characteristics of velocity, turbulent kinetic energy and turbulent dissipation profiles persisted; these would represent the incoming flow to the turbines in D5b. Finally, a comparison was made with flow profiles from other models of the Sound of Islay and with actual ADCP measurements from the sound itself. Good agreement was found with both.

1.2 Acceptance criteria

The acceptance criteria for this report are:

1) **Code Saturne input and output files for the simulations described in this report**.

   These are on the accompanying CD; a README file in the root directory of the CD describes the contents in full.

2) **That the report describes the following, for unsteady turbulent flow conditions:**

   a) The reasoning and justification of the tidal site characterisation and the validation of the resulting model configuration.
   b) The flow characteristics simulated to represent various stages of the tidal cycle and the configuration of those within Code Saturne.
   c) Any caveats and general directions for the work contained in this report to be used within WG3 WP2 D5b.

2. Aims

The primary goal of deliverable 4 (D4) is to enable the work in D5b, where a farm of tidal turbines is simulated within a tidal channel. It does this by providing a validated methodology for simulating a tidal channel at various stages of the tidal cycle, which can be directly applied to D5b. The model was constructed at the mesoscale level, over the volumes that would be expected to simulate a tidal turbine farm, ie. a tidal channel kilometres long. The model was developed within the computational fluid dynamics (CFD) software Code Saturne, using unsteady RANS $k-\varepsilon$ turbulence modelling.

More specifically, the aims of D4 are:

1. **Model dimensions**. To determine the size of model required to investigate mesoscale flow.
2. **Boundary conditions**. To develop appropriate boundary conditions for the model, ie.
   a) The velocity profile for the inlet.
   b) Turbulence boundary conditions.
3. **Mesh characteristics**. This includes:
   a) As a variety of mesh cell types can be used within Code Saturne, the cell types best suited to modelling channel flow – a large aspect ratio problem – will be determined.
   b) The flow characteristics can be affected by mesh resolution, so the best balance between accuracy and computational complexity will be found.
4. **Code Saturne settings**. Code Saturne has a variety of options available to control the solution, which can affect numerical stability. These will be detailed so that future tidal channel simulations can be set up quickly and effectively. This will include noting any 'gotchas', ie. any features or bugs that are not evident from reading the Code Saturne manual.

3. Model parameterisation

3.1 Simulation domain

The model tidal channel had to be large enough to allow mesoscale flow to be represented and for that flow to be fully developed. Broadly speaking, the Sound of Islay was used as a template, since it represents a well-defined, semi-closed environment. It is a relatively straight, 18 km long strait between the islands of Islay and Jury off the West Coast of Scotland. It is 1 km-2 km wide for most of its length (see Figure 1).

Figure 1. Map of the Sound of Islay. As indicated, the sound is 1 km wide at its narrowest point.

However, a three-dimensional numerical model of the entire sound would be extremely computationally demanding and beyond the scope of this deliverable. It is only necessary to construct a model large enough to show that mesoscale sites can be modelled and give the means to do so. Therefore, driven by pragmatism, we will utilise a three-dimensional domain of reduced size, as shown in Figure 2.

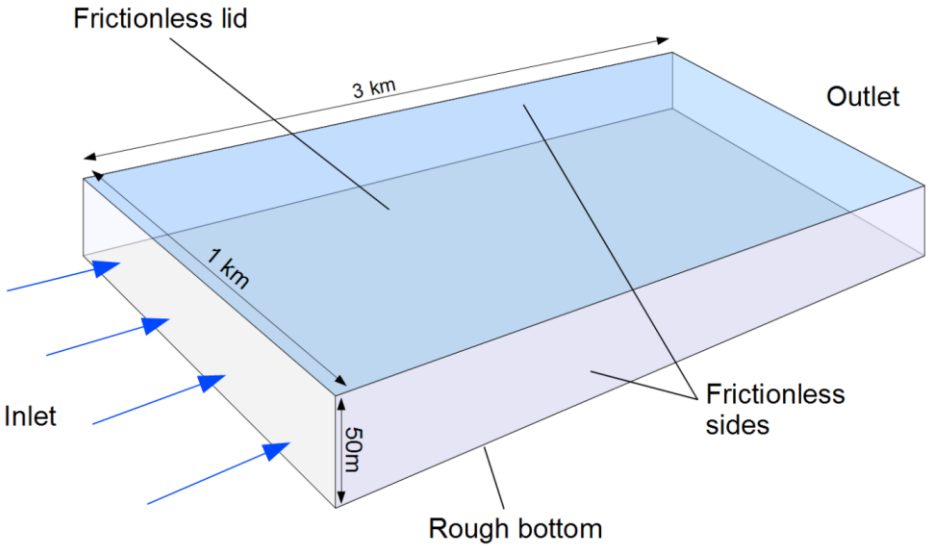

Figure 2. Idealised view of the three-dimensional tidal channel domain. For clarity, the width and length of the channel in the drawing have been reduced.

At 1 km wide and 50 m deep, the idealised domain closely matches the width and depth of the site in the Sound of Islay where Scottish Power Renewables' proposed tidal array is to be constructed [1] (pp. 2). After several test simulations repeatedly extending the channel, 3 km was found to be long enough to allow the turbulent tidal flow to develop fully. It should be noted that, for tidal array simulations, the channel shall have to be extended to 5 km, so that the wakes behind the array can be modelled. This will be done in D5b.

3.2 General Code Saturne settings

This section details the general settings used within all the Code Saturne simulations and explains the reasoning behind them. This should facilitate easy re-creation of tidal channel simulations, even without the original XML files. Unless otherwise indicated, these settings are what the Code

Saturne User Guide [4] calls L1 (level 1) options: ie. they can be changed through the Code Saturne GUI. The Code Saturne option key is in brackets, which can be found in section 9 of the user guide if more details are required.

3.2.1 Physical parameters

Name	Keyword	Value	Explanation
Density	*IROVAR*	1020 Kg/m^3	Density of seawater at 20ºC near surface.
Dynamic viscosity	*IVIVAR*	0.001 Na.s	Dynamic viscosity at 20ºC.

Table 1. List of physical parameters.

3.2.2 Numerical parameters

Name	Keyword	Value	Explanation
Flow algorithm	*IDTVAR*	Unsteady	RANS unsteady state numerically stable; also D5b will use unsteady RANS, so more appropriate choice.
Turbulence model	*ITURB*	k-epsilon	k-ω turbulence modelling buggy in Code Saturne with rough walls: see Section 3.4.3 and [9] for further explanation.
Initial velocity	-	0 m/s	No initial profile assumed; allow channel velocity profile to develop through bottom drag.
Initial turbulence	-	k=6.0x10^{-4} m^2/s^2 ε=1.6x10^{-4} m^2/s^2	A small degree of initial turbulence was found to increase numerical stability: no effect on eventual levels of turbulence.
Unsteady flow algorithm management	-	Variable in time and uniform in space	Default values used for Max. CFL no., Max. Fourier no, etc. except NTMABS (see below).
Number of iterations	*NTMABS*	10000	Sufficient number of iterations for flow to fully develop and become statistically stable. Repeated testing showed this to be a sufficient period for statistically stable flow to develop.
Equation parameters/ scheme (VelocityX, VelocityY, … Dissip)	*ISCHCV*	SOLU	Second-order upwind scheme found experimentally to give greater numerical stability.
Gradient calculation method	*IMRGRA*	Least sq. method over extended cell neighbourhood	Improves numerical stability with strong vertical velocity gradients for slight increase in CPU usage.
Output Control/Post-processing	*NTCHR*	Post-processing every 10 time steps	Gives sufficient time-stepped field data towards end of simulations to allow averages to be calculated. Total disc usage found to be ~30Gb (For every 1 time steps, this increases to 300Gb)
Number of parallel cores	*(see SCRIPTS/ runcase qsub script)*	32	Number of cores to run simulations under MPI. Simulations take approximately 10 hours.

Table 2. Numerical parameters used within Code Saturne in every simulation.

3.3 Mesh configuration

The mesh for the channel domain was generated using GMSH [2], a widely available open-source meshing program capable of generating structured and unstructured meshes using tetrahedral, quadrilaterals or hexahedra cells.

The cell type and aspect ratio of the cells had to be carefully chosen as, whilst Code Saturne can use structured meshes, unstructured meshes and all the above cell types, from experience, the choice can drastically affect solver stability. Manchester's online notes on Code Saturne [3] advise using

elements (in decreasing order of stability) of shape: '*cubes, bricks, hex, prisms, tet*' and that '*keep in mind that regular tetrahedral are better than ill-shaped hexahedra*'. This turns out in practice to mean that anything but a regular quadrilateral mesh is prone to pressure convergence issues after a few iterations.

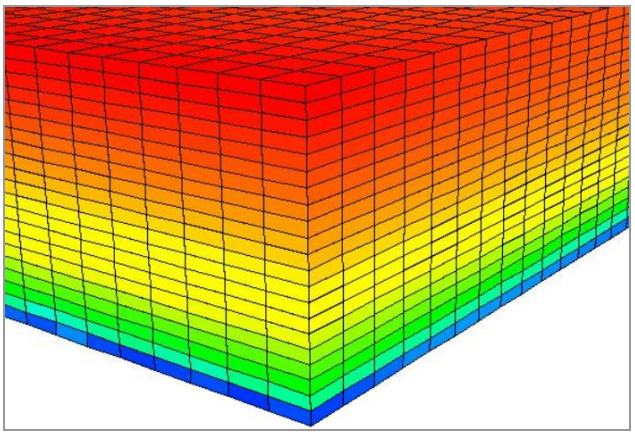

Figure 3. Corner of a tidal channel mesh using an aspect ratio of 3.2 .

The only parameter left, therefore, is the aspect ratio of the cells. The same document [3] advises to avoid aspect ratios larger than 3. However, larger aspect ratios are desirable in our case for computational efficiency, due to the simulation domain being wide, long and relatively flat with little vertical motion flow – shorter, broader elements represent vertical gradients. The issue of cell aspect ratio versus computational efficiency will be investigated further in section 4.1.

3.4 Boundary conditions

3.4.1 Bottom roughness

We assume that our channel model has a bottom roughness, which represents the effect of friction caused by an uneven, rocky layer on the seabed. This can be set within Code Saturne as part of a rough wall boundary condition, with the roughness prescribed as a roughness height, z_0, through the user interface as shown in Figure 4.

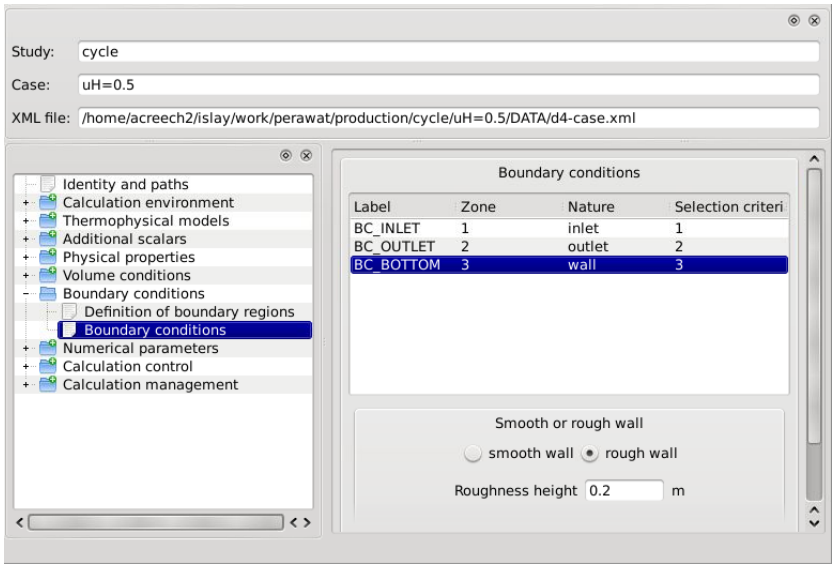

Figure 4. Selecting bottom roughness in the Code Saturne GUI.

Choosing a realistic value of z_0 for an idealised tidal channel is not a straightforward task. Since no estimates are available for the Sound of Islay, the site that closest resembles our model, are known, a review was conducted of previous estimates for tidal channels. Prior work by the author has used $z_0 = 0.4\,\mathrm{m}$ [5], which was based upon Yamaguchi et al's estimates for the Kanmon Strait [8]. However, there is a degree of variability in roughness lengths calculated elsewhere: You [6] estimates z_0 to vary from 0.01 cm – 0.1 m, whereas Lueck and Lu [7] calculate the roughness for the Cordova channel to vary between 0 and 0.1 m.

Given the large variation in possible values for z_0 and that the smaller values (<<1cm) clearly correspond to sediment, which we have assumed does not exist on our seabed, we have opted for a middle, realistic value of $z_0 = 0.2\,\mathrm{m}$.

3.4.2 Velocity profile

The velocity profile is set at the inlet shown in Figure 2, as a Dirichlet condition. This takes the form of a standard logarithmic profile for turbulent flow, ie.

(1) $$u(z) = \frac{u_\tau}{\kappa} \ln\left(\frac{z}{z_0}\right)$$

Where $u(z)$ is the x-component of the water velocity at height z above the seabed, κ is the Von Karman constant ($= 0.41$), and u_τ is the friction velocity. The y and z components of velocity are zero.

It should be noted that we are neglecting the viscous sub-layer here, as it is extremely small compared to the turbulent layer, and will not have much impact on the fully-developed flow downstream in the CFD simulation. Hence, the boundary velocity profile must only qualitatively represent the flow overall. As a result, where $z < z_0$, we set $u = 0$.

To calculate u_τ, as we already know z_0, we must specify u at a known height at the boundary. A sensible choice would be at the presumed hub-height, z_H, of the tidal turbines to be modelled in D5b. If we say $u_H = u(z = z_H)$, then we can write the frictional velocity as

(2) $$u_\tau = u_H \kappa \left[\ln\left(\frac{z_H}{z_0}\right)\right]^{-1}$$

In this case, we set $z_H = 40\,\mathrm{m}$. In the main suite of simulations, we will run with the values $u_H = \{1, 2, \ldots 4\,\mathrm{m/s}\}$ to represent at relatively slow-moving currents (1 m/s), through to full-flood (4 m/s). The velocity log profile will be set via the **`usclim.f90`** routine in Code Saturne.

Note

H is simply the notional height at which we specify u: whether it corresponds directly to the actual hub-heights is not of critical importance, only being done so for convenience.

3.4.3 Turbulence boundary conditions

Turbulence is injected into the simulation at the inlet boundary to simulate the turbulence upstream of the model channel. This utilises the $k-\varepsilon$ two-equation RANS turbulence model within Code Saturne, not $k-\omega$ as specified in previous deliverables, due to a documented bug in $k-\omega$ turbulence modelling within the software when using rough walls [9], which leads to numerical stability issues. There are two approaches to doing this, which are described below.

Wilcox turbulence profile

This is currently utilised in the turbine simulations in D5a, as described in Wilcox [10], which describes turbulence boundary profiles for k (the turbulent kinetic energy) and ε (the turbulent dissipation) as:

(3) $$k = \frac{u_\tau^2}{\sqrt{C_\mu}}$$

And

(4) $$\varepsilon = \frac{u_\tau^3}{\kappa z}$$

Where C_μ is a known constant [10], and predetermined as $C_\mu = 0.09$.

There are two issues with this approach. Firstly, it is not known whether this is an appropriate boundary condition when applied to mesoscale turbulent flows; secondly, the level of turbulence (the turbulence intensity) cannot be varied to suit different scenarios.

Flat turbulence profile

Fortunately, Code Saturne provides us with an alternative should this first approach not be appropriate. Within the Code Saturne GUI, the turbulence at the inlet can be specified by two parameters: the turbulent intensity (TI), and the hydraulic diameter, a term commonly used in describing turbulent channel flow, as shown in Figure 5.

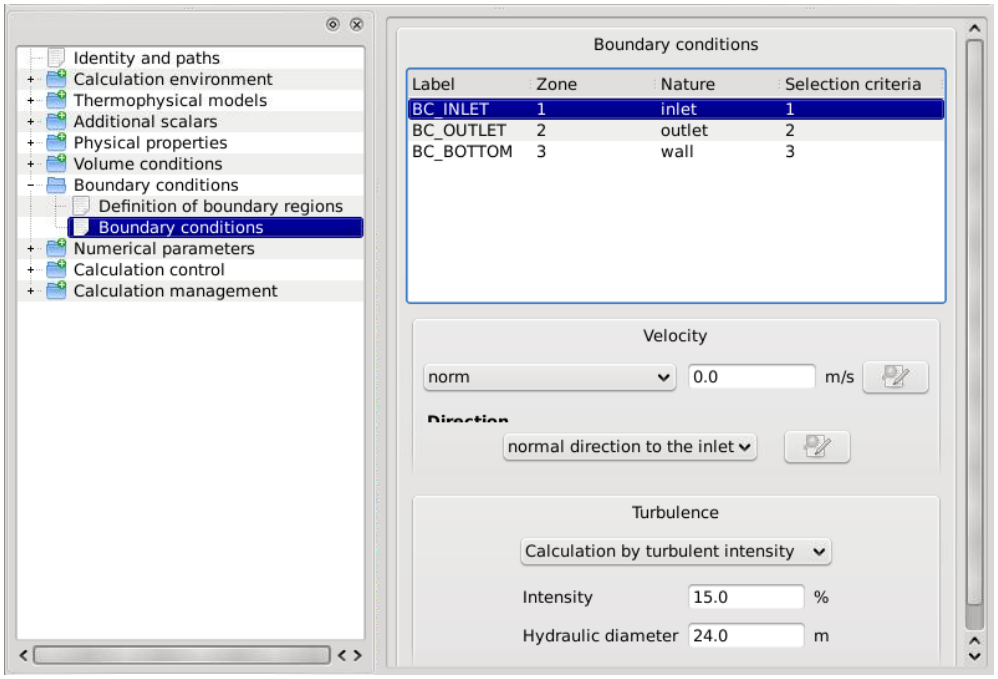

Figure 5. Setting turbulence boundary conditions at the inlet within the Code Saturne GUI.

To choose an appropriate value for turbulence intensity, we can look to measurements from sites which broadly match our idealised tidal channel. Work at Heriot-Watt [12] has shown a streamwise TI[1] of 12-15% at the EMEC test site at the Falls of Warness in Orkney, whereas Li et al [13] have calculated it to be 25% for East River, New York. Milne et al [11] conclude that turbulence intensity is particular to each site; they themselves calculated the turbulence intensity from ADCP measurements at a site in the Sound of Islay to be 12-13%. Therefore, given these range of values, and given that the Sound of Islay most closely represents our channel, a realistic TI for the model would be 15%.

There are several definitions of the hydraulic diameter D_H; we shall use the most common definition, ie.

(5) $$D_H = \frac{A}{P}$$

Where A is the cross-sectional area of the channel, and P is the wetted perimeter (ie. the perimeter of the cross-section that contains water). In this case $P = width \times depth$, which gives us a hydraulic parameter of $D_H \approx 24\,\mathrm{m}$.

4. Trial simulations

4.1 Mesh resolution

In these particular test simulations, the main goal was to find the optimum balance between mesh resolution and simulation accuracy; specifically, how many vertical levels were required in the mesh to give an accurate representation of the vertical velocity profile. The flow speed at hub-height was defined as $u_H = 2.0\,\mathrm{m/s}$, and a flat turbulence profile was prescribed at the boundary as described in section 3.4.3.

[1] Note that we are only dealing with *streamwise* turbulence intensity. Turbulence in tidal flows is often anisotropic, but given that RANS $k-\varepsilon$ only deals with isotropic descriptions of turbulence, we must neglect the ancillary components.

4.1.1 Cell shapes

Quadrilateral cells were used exclusively in a structured mesh, since this mesh configuration is rated highly for stability with Code Saturne [3]. The cell types are listed below Table 3.

Label	Type	Dimensions	Aspect ratio	No. cells
coarse	quadrilateral	10m x 10m x 5m	2	334411
fine	quadrilateral	8m x 8m x 2.5m	3.2	994896

Table 3. Cell and mesh configurations used in resolution tests.

4.1.2 Results

To see how the flow structure was affected horizontally and vertically by a change in resolution, a set of horizontal profiles and vertical profiles of velocity, turbulent kinetic energy (TKE) and turbulent dissipation, were plotted for both the coarse and fine mesh tests. The horizontal plots are displayed first below, followed by the vertical plots. These plots were extrapolated from the centre at of the channel (ie. 500 m from either side), and averaged over the last 200 iterations to ensure unsteady fluctuations were averaged out.

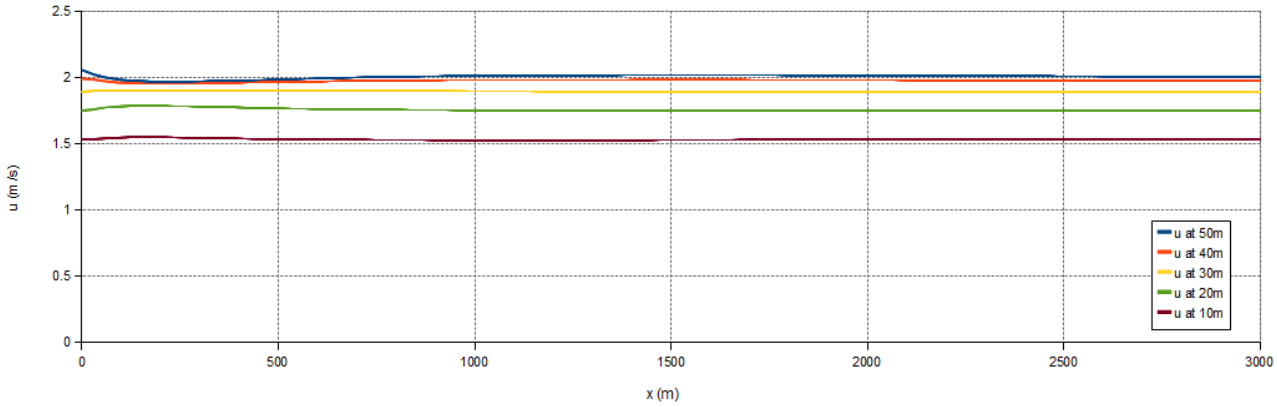

a)

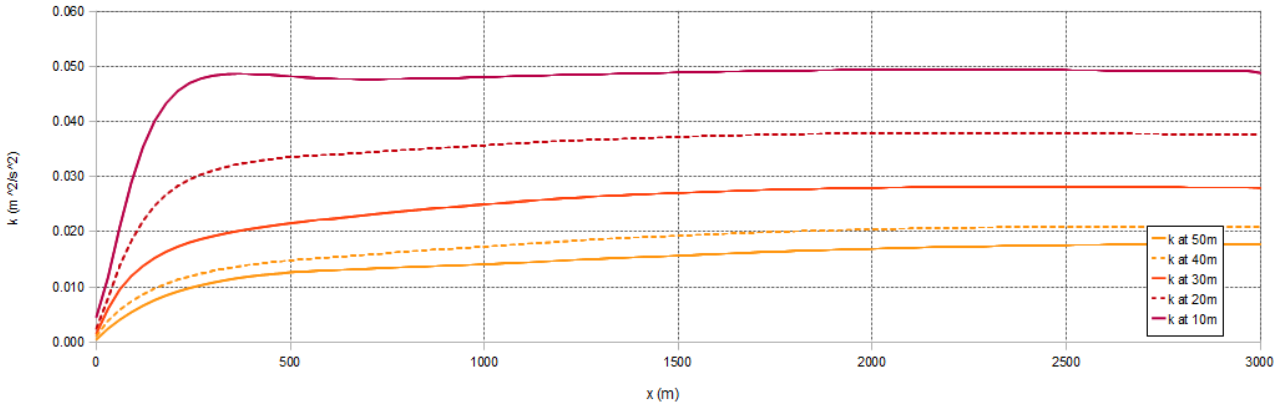

b)

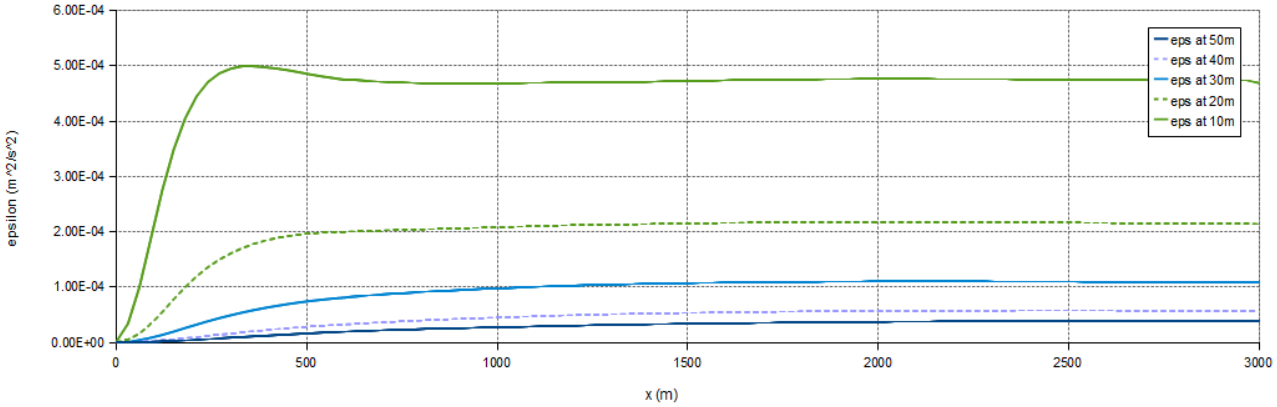

c)

Figure 6. From the coarse profile mesh test. Time-averaged horizontal profiles (x=distance downstream from inlet) at varying heights for: a) flow speed b) turbulent kinetic energy, and c) turbulent dissipation.

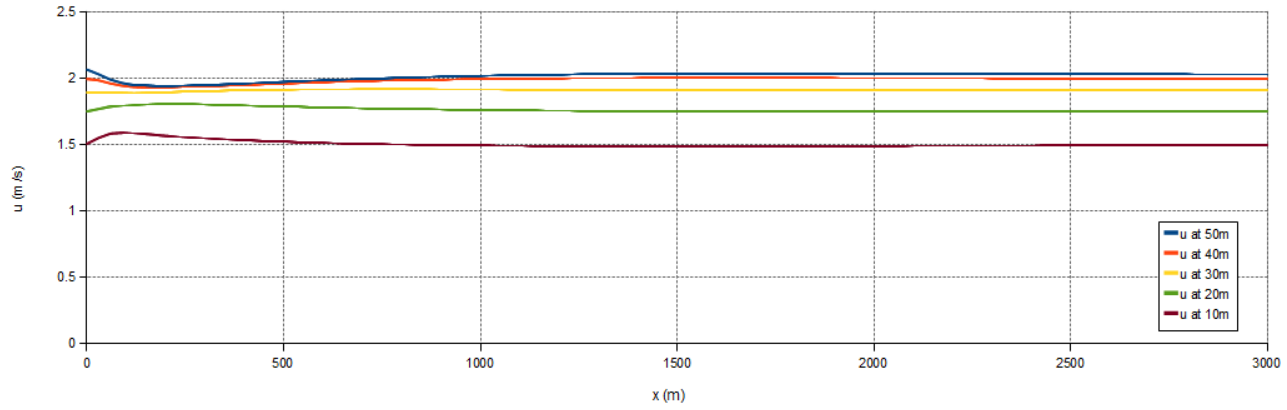

a)

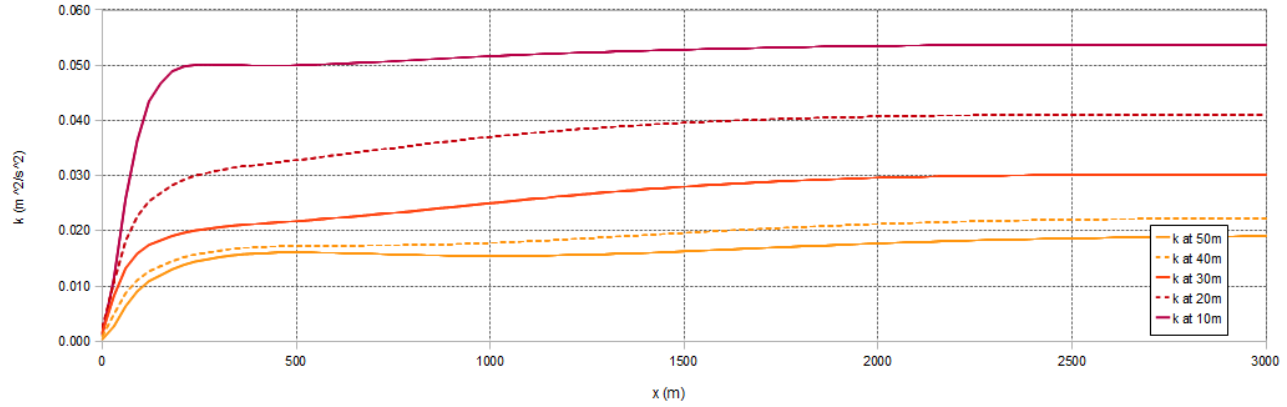

b)

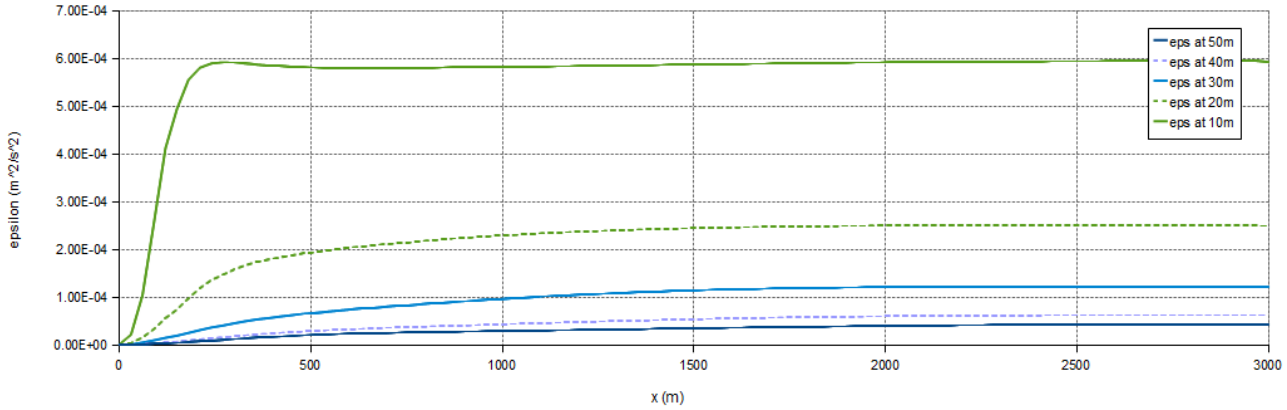

c)

Figure 7. From the fine mesh test. Time-averaged horizontal profiles (x=distance downstream from inlet) at varying heights for: a) flow speed b) turbulent kinetic energy, and c) turbulent dissipation.

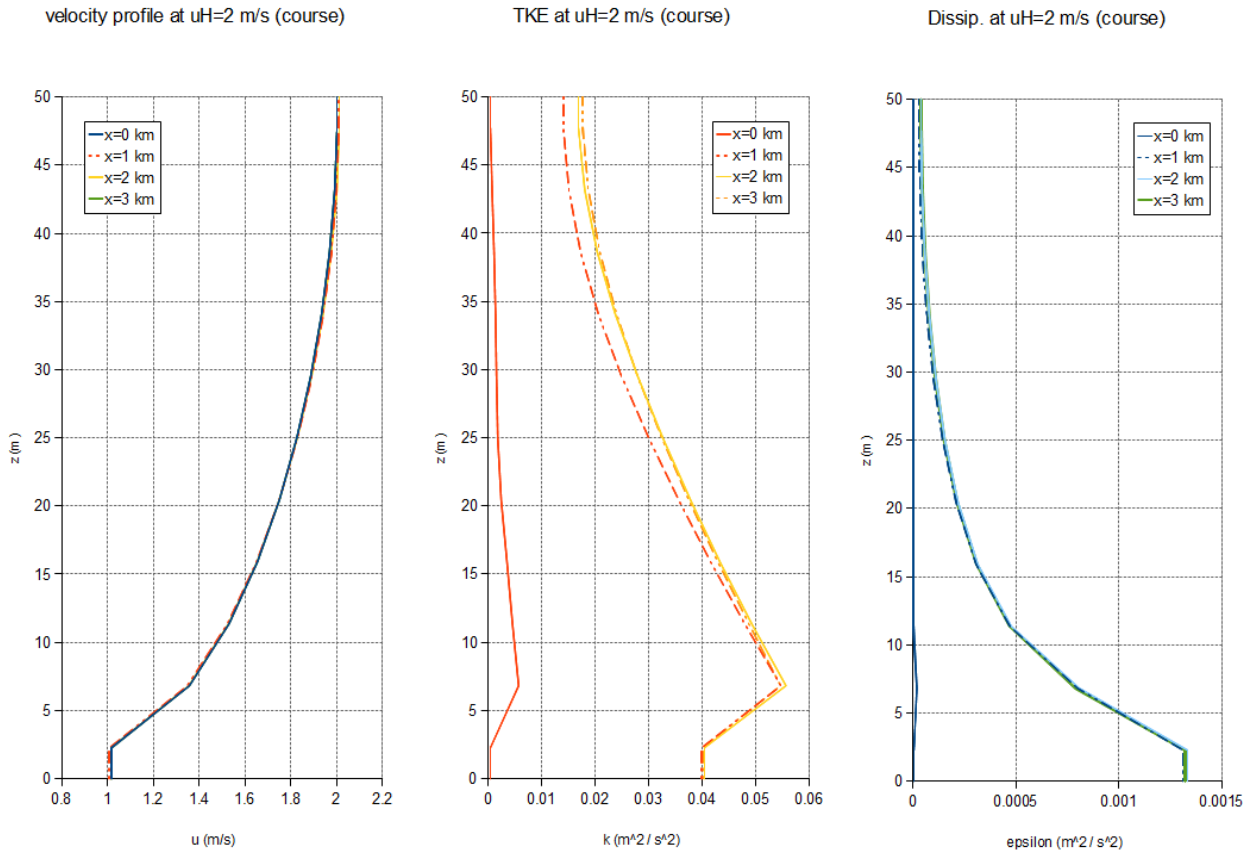

a)

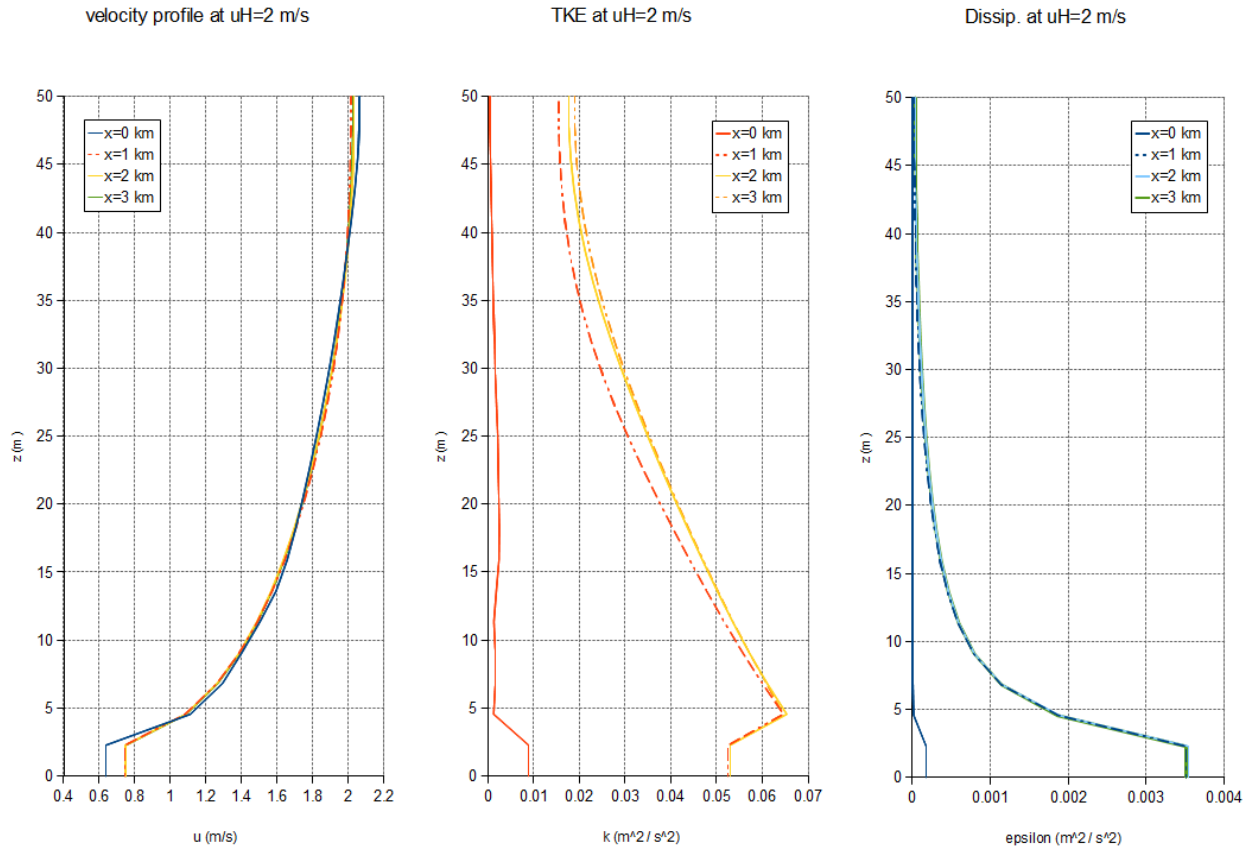

b)

Figure 8. Comparison of vertical profiles for flow speed, turbulent kinetic energy (TKE) and turbulent dissipation for: a) coarse mesh and b) fine mesh.

4.2 Turbulence inlet profiles

These tests were conducted to decide which type of turbulence boundary condition was appropriate for use in tidal channel simulations. A coarse resolution was used for convenience, as it was expected to demonstrate trends in fluid behaviour with little computational effort. As with the mesh resolution tests, $u_H = 2.0\,\mathrm{m/s}$.

4.2.1 Boundary types

Two types of boundary were tested, as discussed in section 3.4.3; these are listed below in Table 4.

Label	Type	Resolution
Flat	TI and hydraulic diameter	Coarse (see Table 2)
Wilcox	Calculated vertical profiles for k and ε. See section 3.4.3, in particular equations (3) and (4).	Coarse

Table 4. Turbulence boundary conditions used.

4.2.2 Results

As with section 4.1.2, to examine flow structure both horizontal and vertical profiles were taken from the centre of the channel. The results were averaged over the last 200 iterations. For brevity, the flat turbulence boundary condition horizontal inlet profiles are not reproduced here. These can be found in Figure 6. For clarity however, the vertical profiles for the same condition are shown in Figure 10.

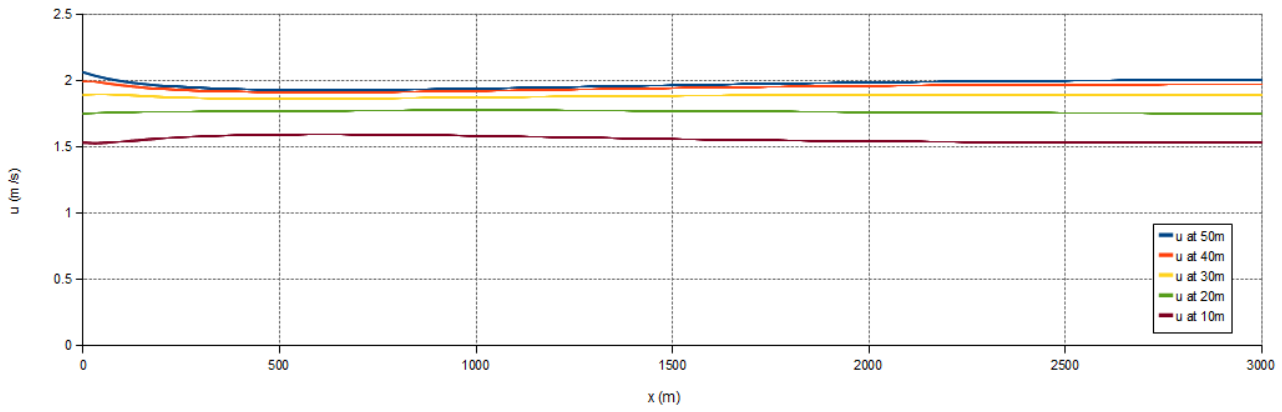

a)

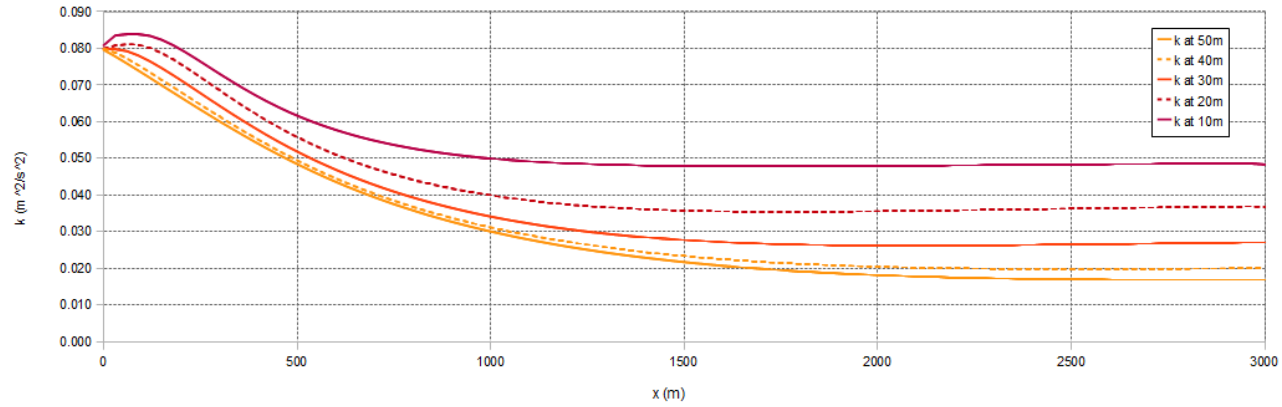

b)

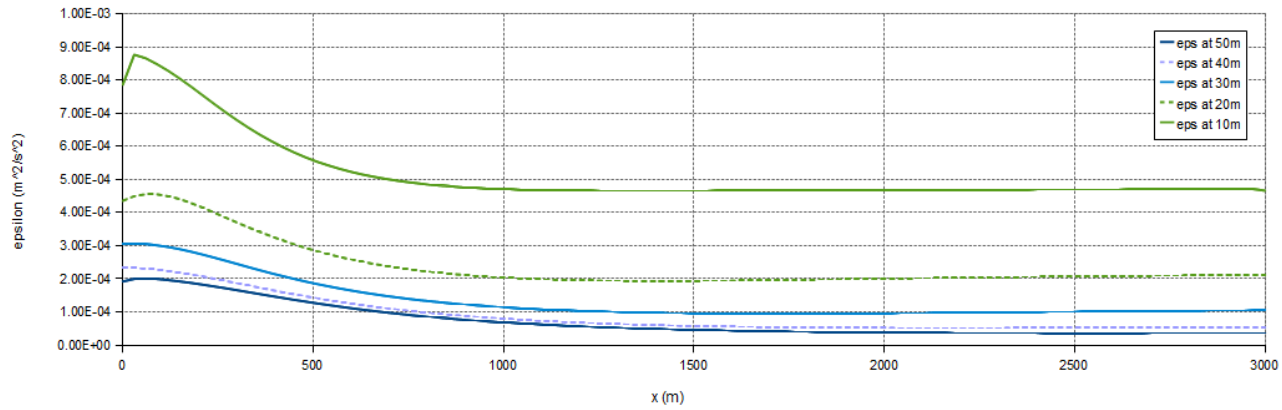

c)

Figure 9. From the Wilcox profile test. Time-averaged horizontal profiles (x=distance downstream from inlet) at varying heights for: a) flow speed b) turbulent kinetic energy, and c) turbulent dissipation.

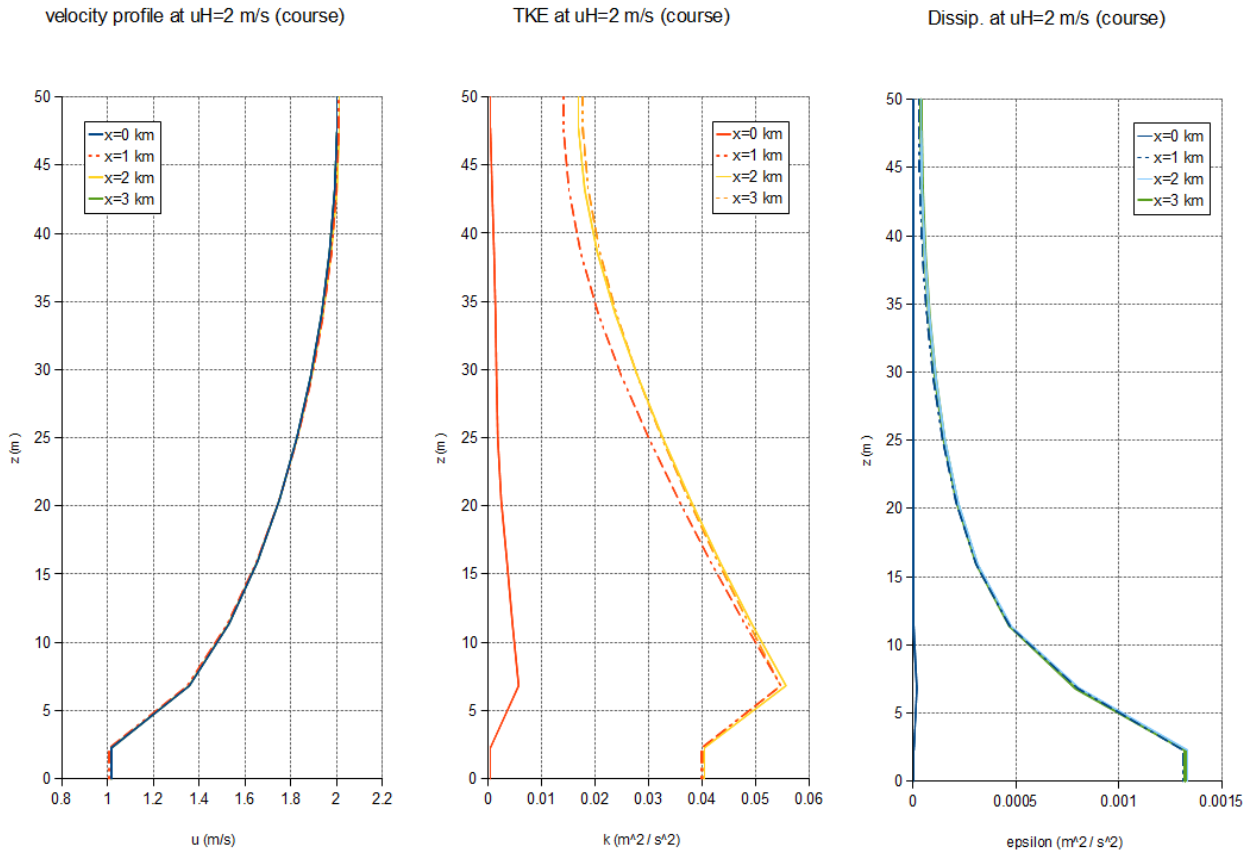

a)

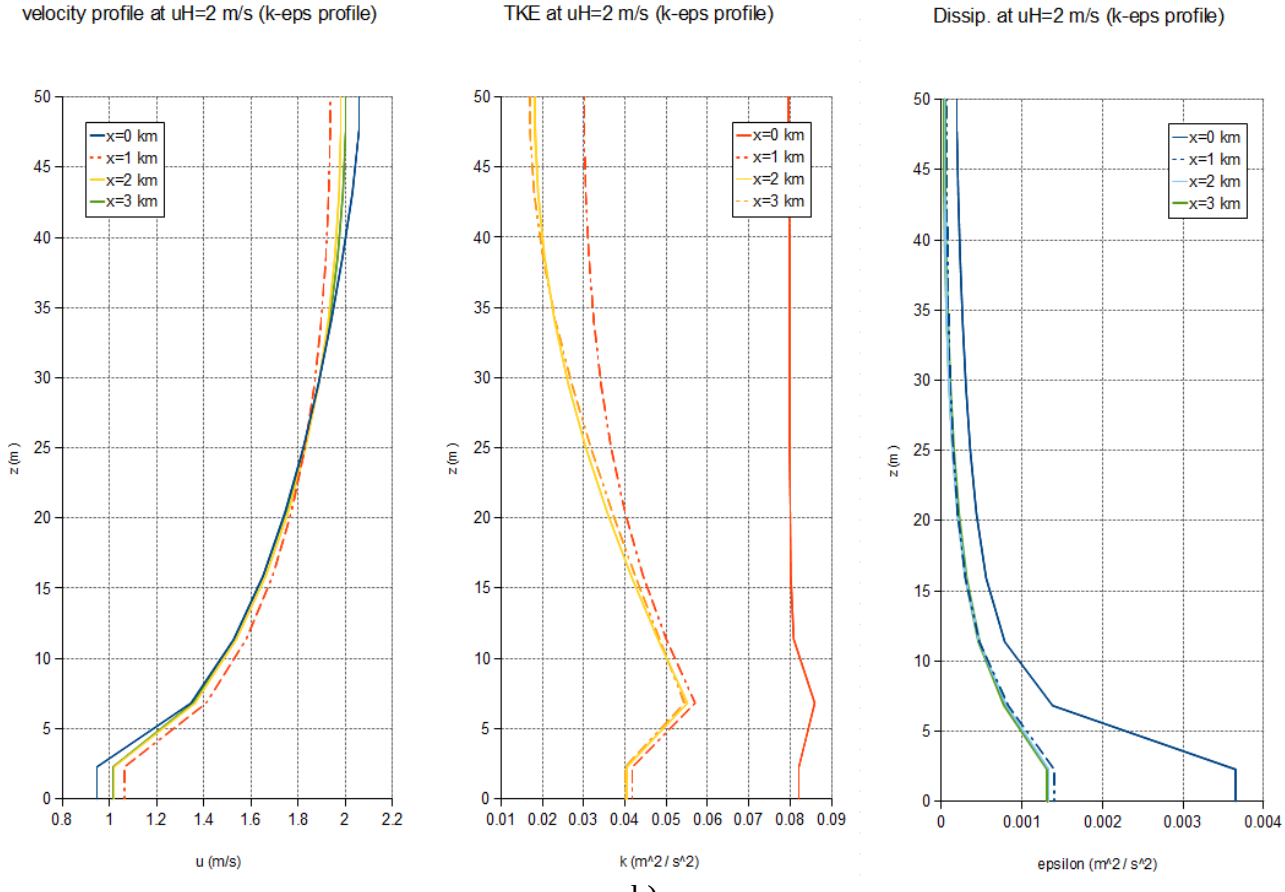

b)

Figure 10. Comparison of vertical profiles for flow speed, turbulent kinetic energy (TKE) and turbulent dissipation for: a) flat turbulence profile (coarse), and b) Wilcox turbulence profiles.

4.3 Analysis

4.3.1 Mesh resolution tests

Comparing the coarse and fine mesh test results, from the horizontal velocity plots in Figure 6a and Figure 7a, there is little difference between the velocity profiles, which are relatively stable after 1km downstream of the inlet. There is some fluctuation with x, but this is around 2%. Moreover, we can see that, at $H = 40\,\mathrm{m}$, the flow speed closely matches $u_H = 2.0\,\mathrm{m/s}$. This can be seen further in the vertical velocity profiles in Figure 8a and b, where the profiles downstream largely maintain the logarithmic profile specified at the inlet. There is some small deviation further downstream in the fine mesh velocity profile (Figure 8b) but this essentially remains unchanged after 1 km downstream of the inlet.

The main differences occur in the turbulent kinetic energy k and turbulent dissipation ε. It should be clear that, from the horizontal TKE profiles in Figure 6b and Figure 7b, the fine mesh produces higher TKE values; looking at the vertical profiles in Figure 8 we can see that this is of the order 18% close to the seabed, and 10% at $z = 25\,\mathrm{m}$. Closer to the surface, there is little difference. A similar story is seen with the turbulent dissipation, which exhibits higher values nearer the seabed: 26% greater at $z = 10\,\mathrm{m}$, and 16% at $z = 20\,\mathrm{m}$. This suggests that mesh resolution affects the unsteady RANS $k-\varepsilon$ turbulence model and that finer meshes effectively produce higher turbulence near the channel bottom. However, these differences become less when approaching hub height and result in a small deviation in the velocity profiles near the seabed. An even finer mesh resolution would show further, smaller improvement, but, as the jump from coarse to fine meshes represented a 3-fold increase in computing resources, the law of diminishing returns applies and so the fine mesh will be taken as an acceptable and practical choice.

4.3.2 Turbulence inlet profiles

Looking at the horizontal profiles for the Wilcox profile test in Figure 9, we can see that in a) the velocity deviates less than 10% from the inlet boundary profile on average, and, by 2 km downstream, the flow speeds from the channel floor to the surface are practically identical to the flat turbulence inlet boundary test in Figure 6. However, the plots for k and ε are in stark contrast: in Figure 9b, k at $z = 10\,\mathrm{m}$ is 0.08 $\mathrm{m^2/s^2}$ and only decays to a stable value when $x = 1500\,\mathrm{m}$; for the profile at $z = 50\,\mathrm{m}$, k again starts at 0.08 $\mathrm{m^2/s^2}$, and takes 1 km longer ($x = 2500\,\mathrm{m}$) to reach a stable value. With Figure 9c, we see a similar story for the turbulent dissipation ε, but with a sharper decay.

The differences between the flat turbulence profile test and the Wilcox profile test are more evident in vertical profiles for both tests in Figure 10. From the flat turbulence test in a) we can see that the velocity profile changes little as it moves progressively downstream, whereas from b) the velocity profile from the Wilcox test is still evolving at $x = 3\,\mathrm{km}$ – the outlet end of the channel. Moving onto the vertical profiles for k and ε, the same pattern is clear: vertical profiles for the flat inlet turbulence test stabilise more quickly than the Wilcox profile test.

It should also be apparent from Figure 6 and Figure 9 that values for u, k and ε in both tests eventually settle down to the same values. The issue of which turbulence boundary conditions to choose then boils down to i) the most efficient use of computational resources, and ii) flexibility. With the Wilcox profile at the inlet, it is clear that any tidal farm simulation would have to start at $x \geq 3\,\mathrm{km}$, whereas the flat inlet turbulence profile is relatively stable in u, k and ε at $x = 2\,\mathrm{km}$. This means that effective 'entry length' – ie. the part of the tidal channel dedicated to allowing the

turbulent flow to become statistically stable, and not used for tidal farm simulations – is 1 km shorter for the flat turbulence profile test. This means less computational resource is required to simulate the tidal channel effectively than the Wilcox profile test. Furthermore, simulating tidal flows of varying degrees of turbulence is relatively straightforward, achieved by simply changing the boundary turbulence intensity in the GUI (see Figure 5). For these two reasons, flat turbulent profiles will be used at the inlet boundary for 'production runs' of the tidal channel simulations.

5. Modelling the tidal cycle

This set of simulations modelled the tidal channel under a variety of flow conditions, from relatively slow flow to full tidal flood. These were then compared with measured ADCP data.

5.1 Flow conditions

For the inlet, the logarithmic velocity profile for turbulence flows was used, as described in equation (1). This was coupled to the flat turbulence inlet boundary condition, described in section 3.4.3 – as opposed to calculated k and ε profiles – with a hydraulic diameter of 24 m and a turbulence intensity of 15%, as also discussed in the same section. The notional hub-height was set to $H = 40\,\mathrm{m}$, with u_H varied as shown below. The mesh resolution was set to "*fine"* as detailed in section 4.1.1, Table 3. All other settings were as described in section 4, Table 2.

u_H (m/s)	H (m)	Velocity profile	Inlet turbulence
1.0	40	Logarithmic	Flat profile
2.0	40	Logarithmic	Flat profile
3.0	40	Logarithmic	Flat profile
4.0	40	Logarithmic	Flat profile

Table 5. Inlet flow conditions used to model the tidal cycle.

5.2 Results

The results here follow a similar approach to sections 4.1.2 and 4.2.2 - horizontal and vertical profiles were taken from the centre of the channel, with results averaged over the last 200 iterations. Figure 11 shows the horizontal velocity profiles for $u_H = \{1, 2, \ldots 4\,\mathrm{m/s}\}$; Figure 13 shows the same, but for the turbulent kinetic energy, k; Figure 13 shows the profiles for the turbulent dissipation, ε. The figures on pages 22 and 23 compare the vertical profiles of each of the simulations.

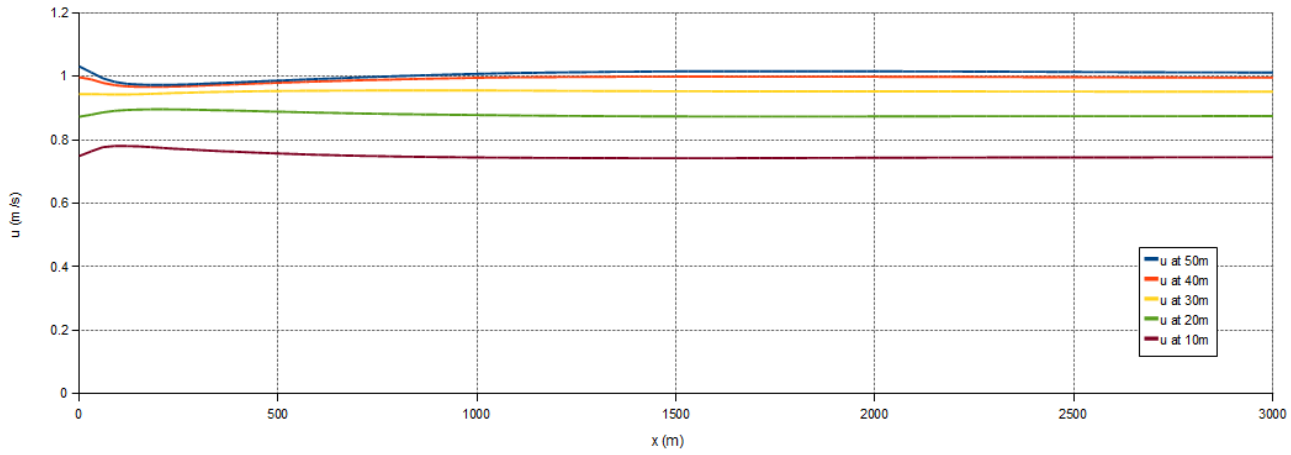

a)

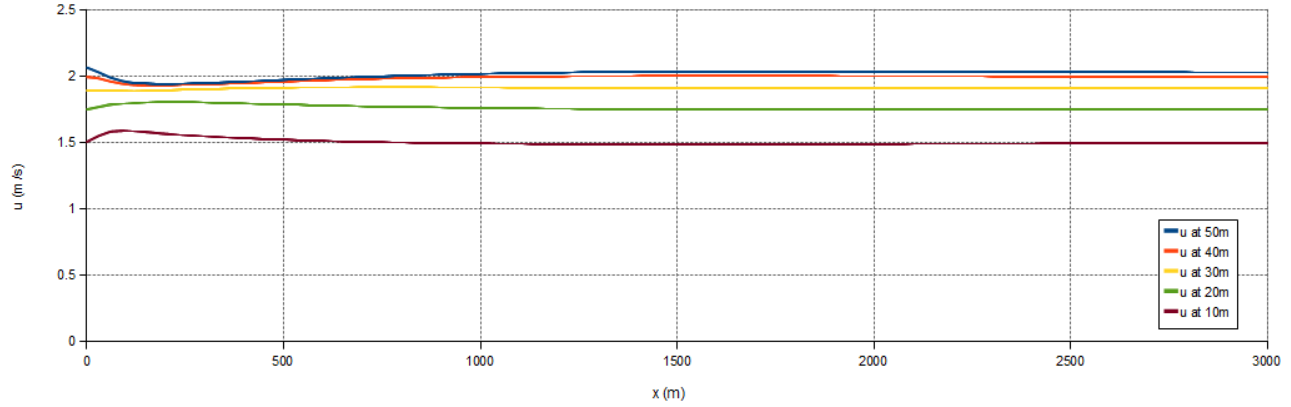

b)

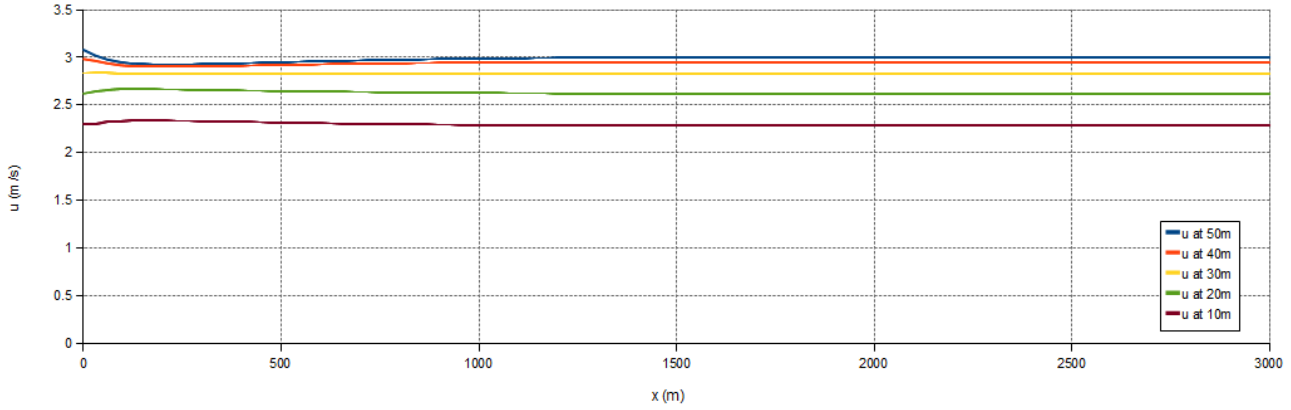

c)

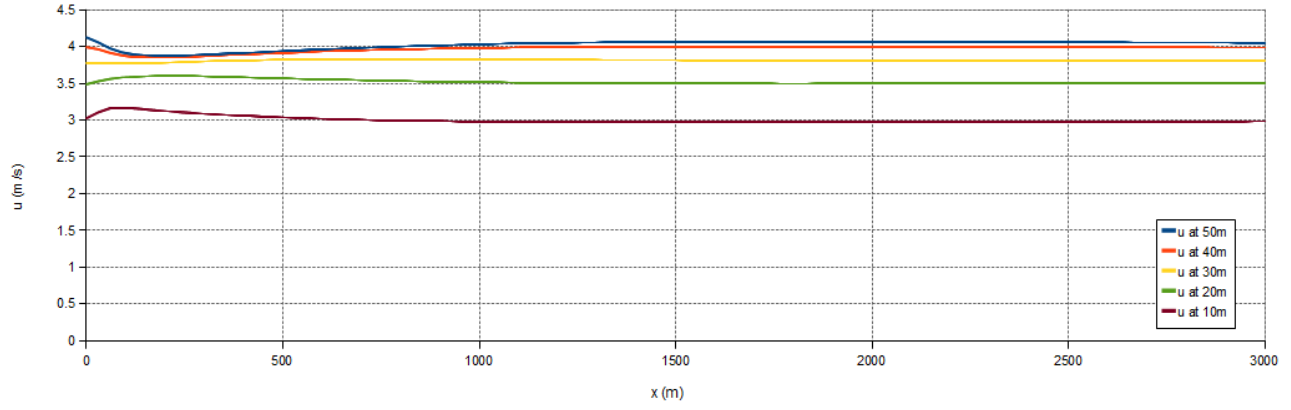

d)

Figure 11. Time-averaged horizontal velocity profiles for: a) uH= 1 m/s, b) 2 m/s, c) 3 m/s, and d) 4m/s.

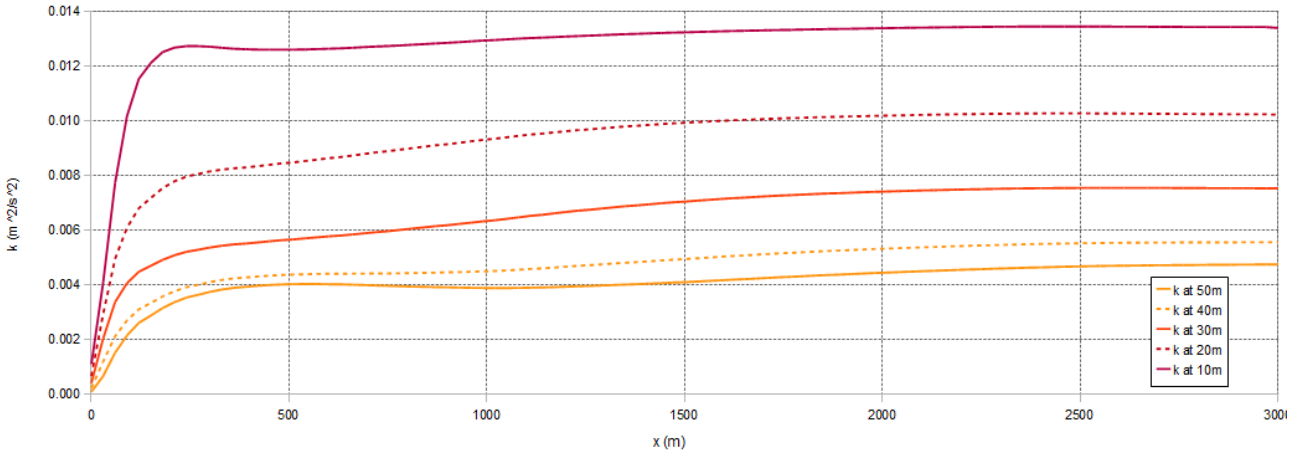

a)

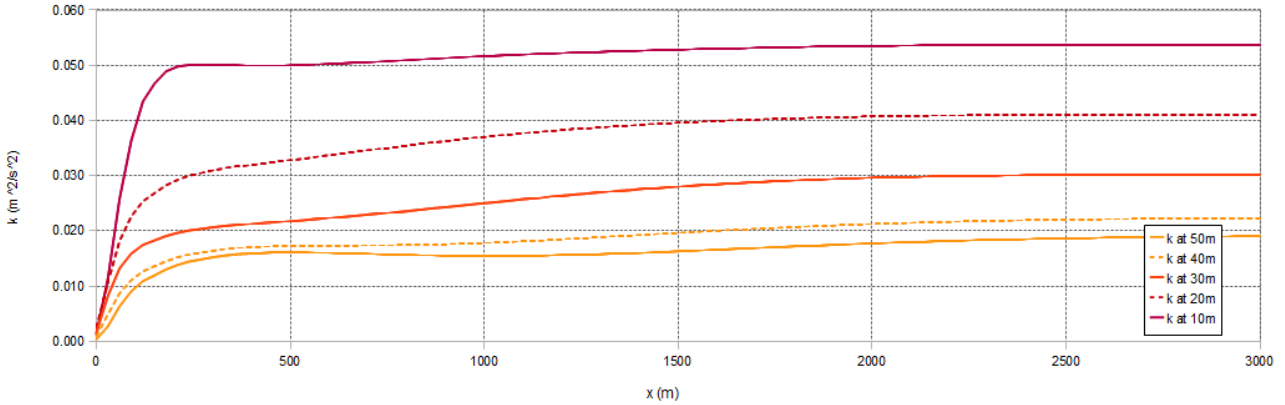

b)

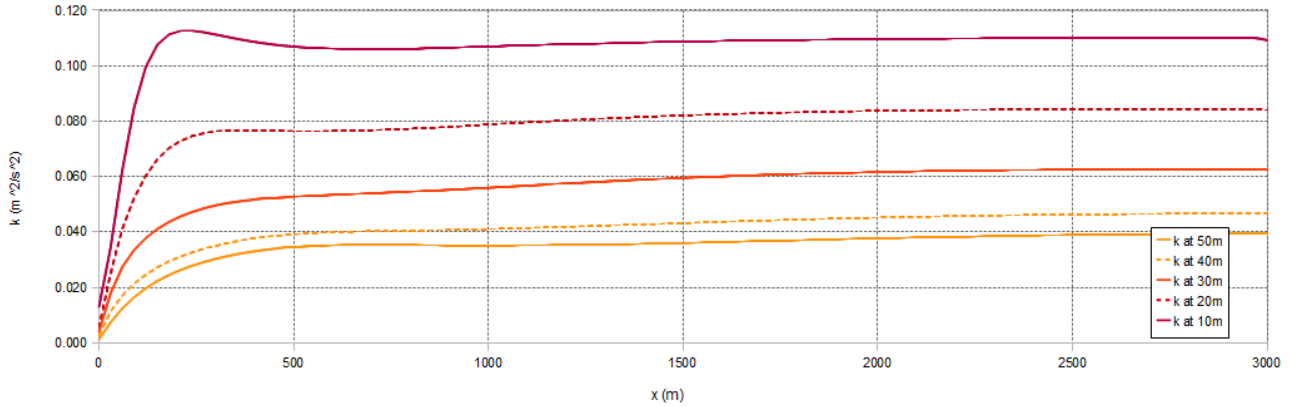

c)

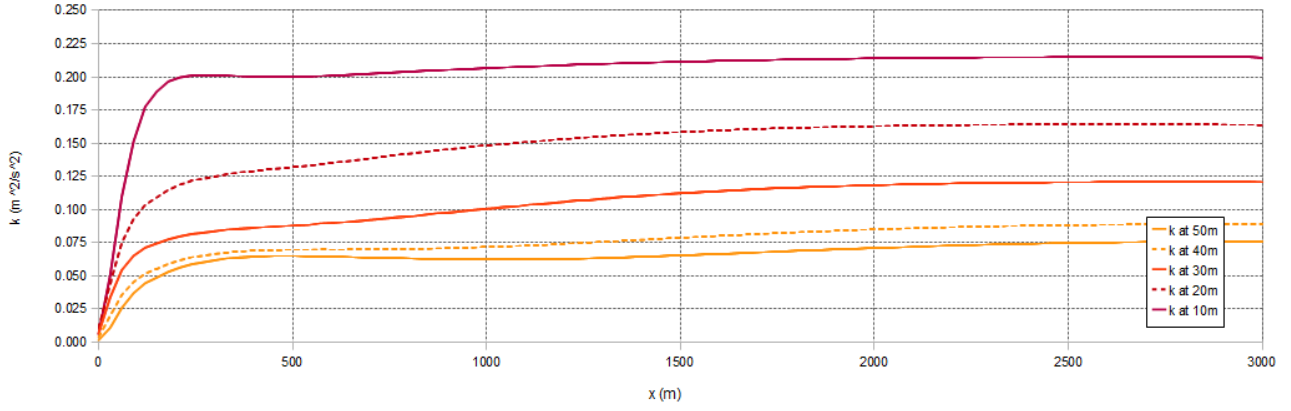

d)

Figure 12. Time-averaged horizontal TKE profiles for: a) uH=1 m/s, b) 2 m/s, c) 3 m/s, and d) 4m/s.

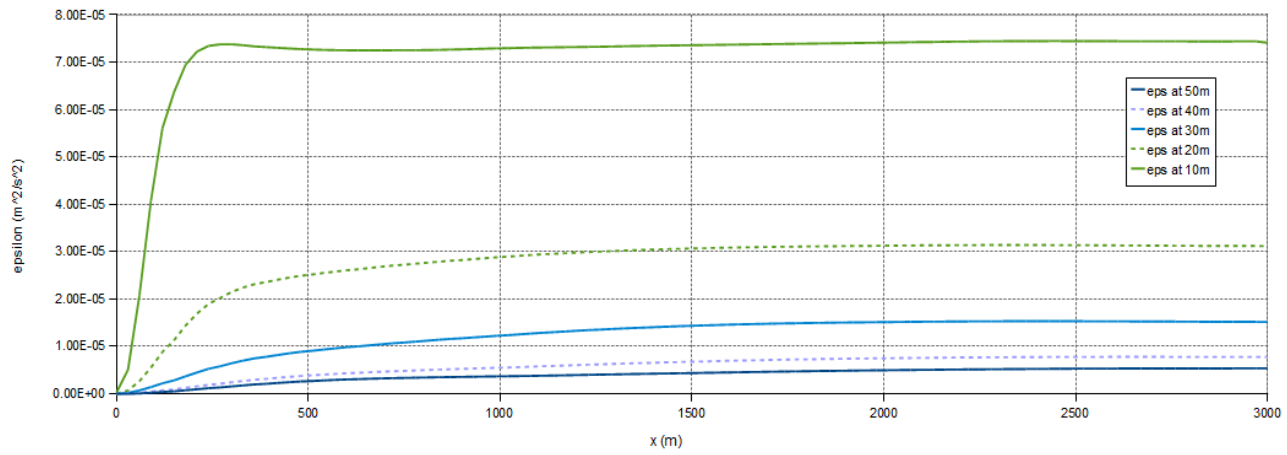

a)

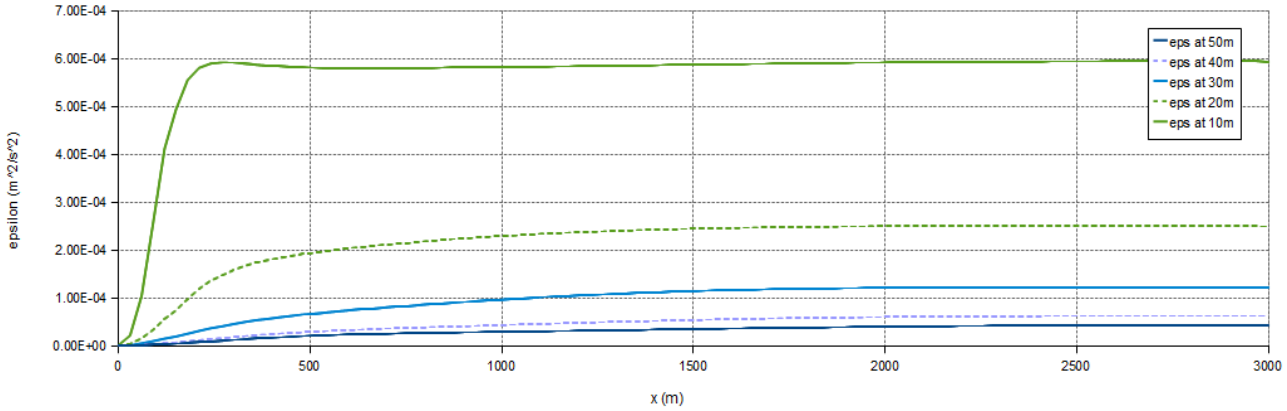

b)

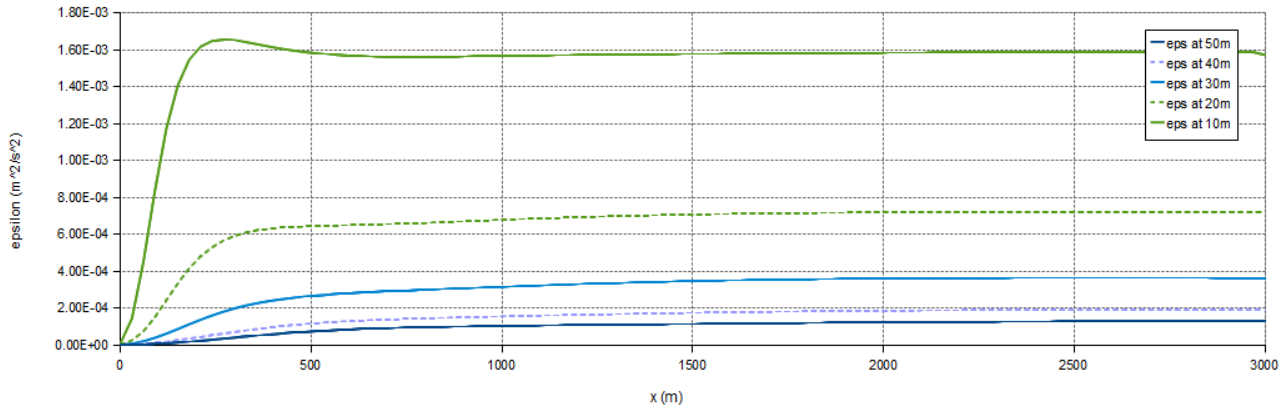

c)

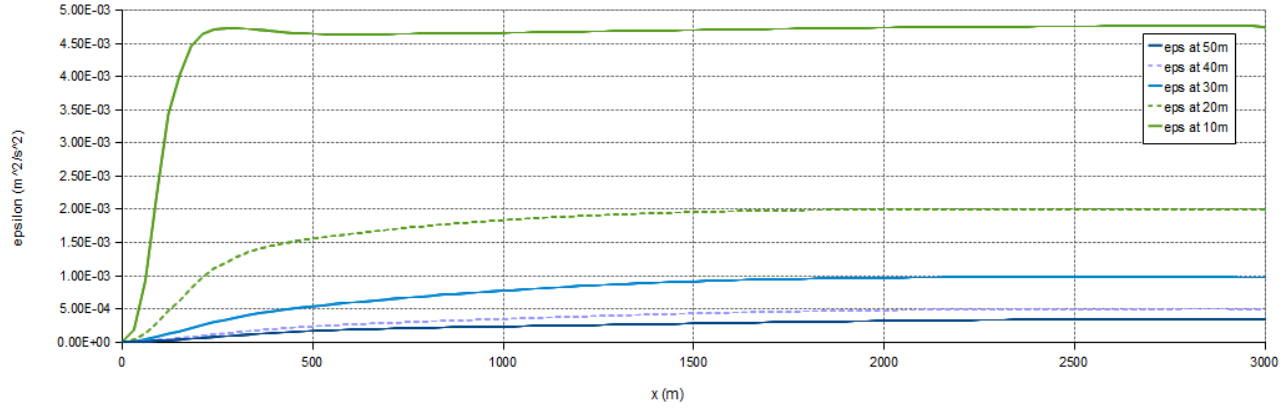

d)

Figure 13. Time-averaged horiz. turbulent dissipation profiles for: a) uH=1 m/s, b) 2 m/s, c) 3 m/s, and d) 4m/s.

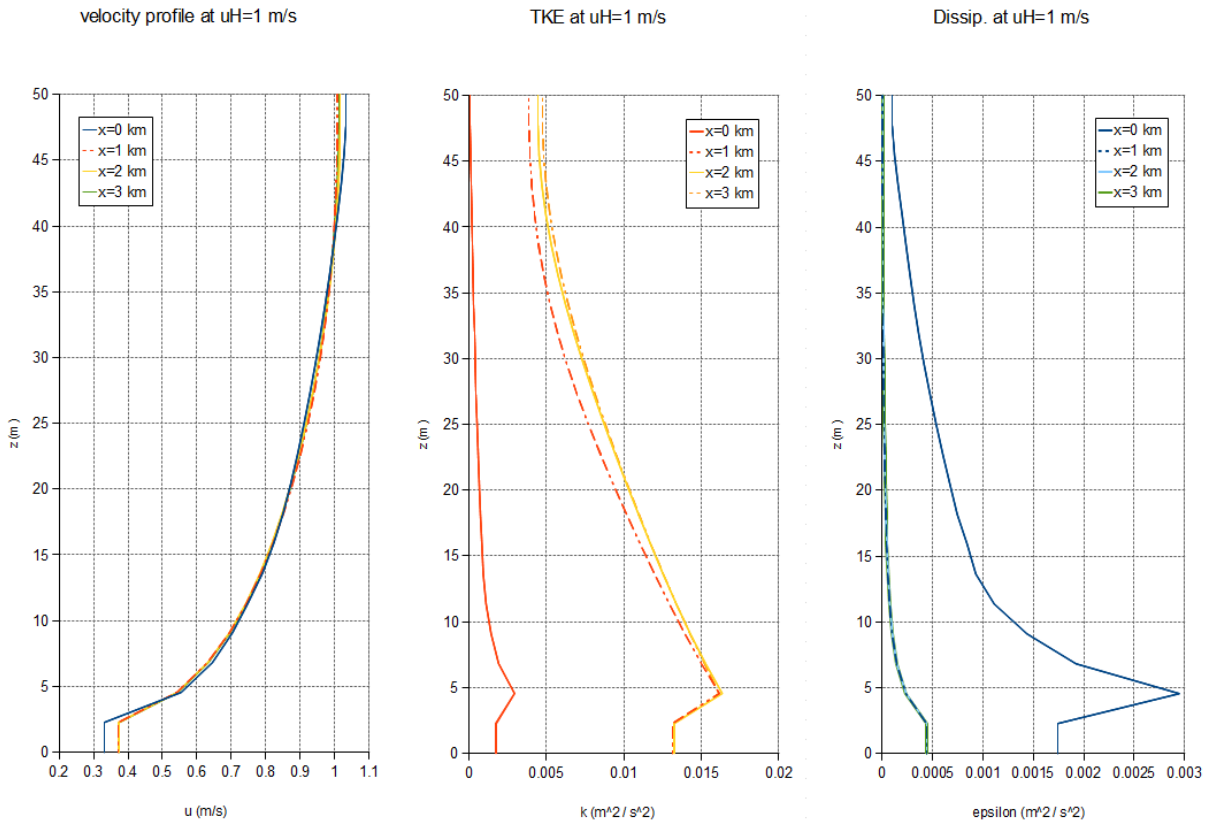

Figure 14. Vertical profile for flow speed, turbulent kinetic energy (TKE) and turbulent dissipation for uH=1 m/s.

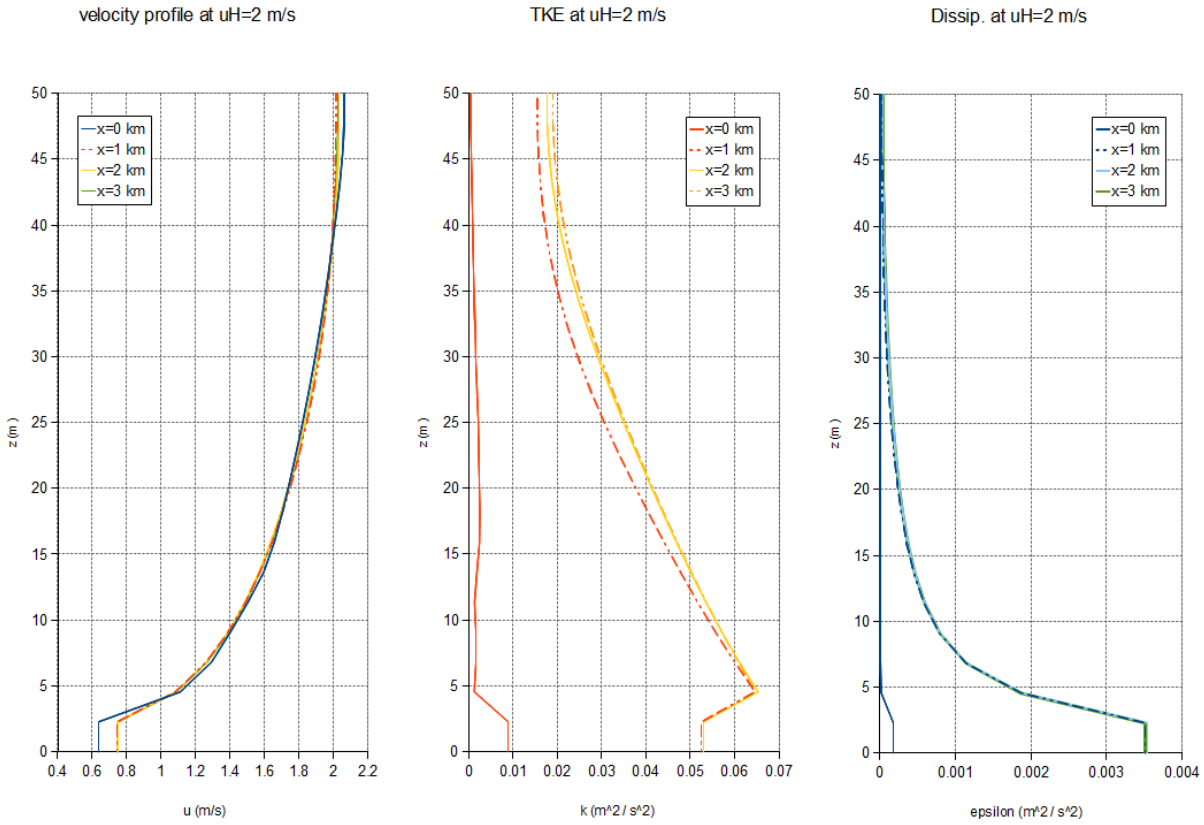

Figure 15. Vertical profile for flow speed, turbulent kinetic energy (TKE) and turbulent dissipation for uH=2 m/s.

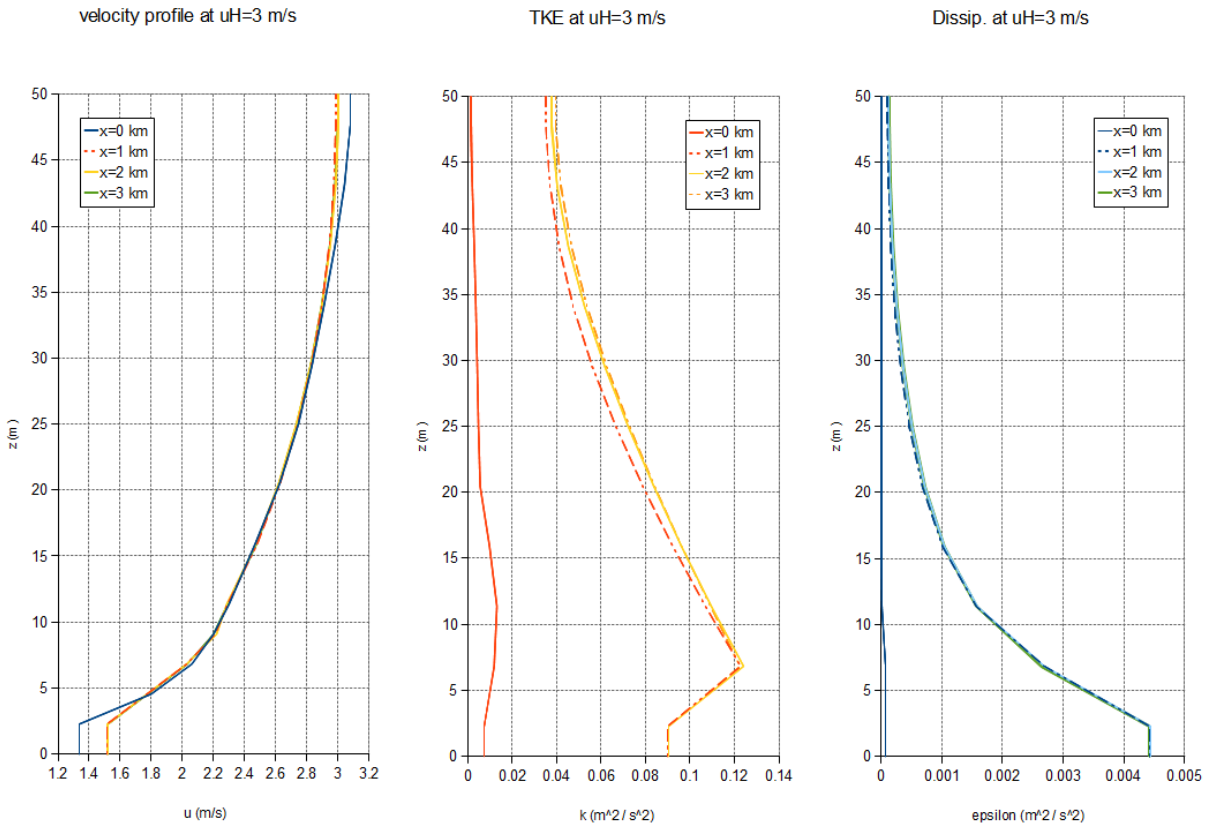

Figure 16. Vertical profile for flow speed, turbulent kinetic energy (TKE) and turbulent dissipation for uH=3 m/s.

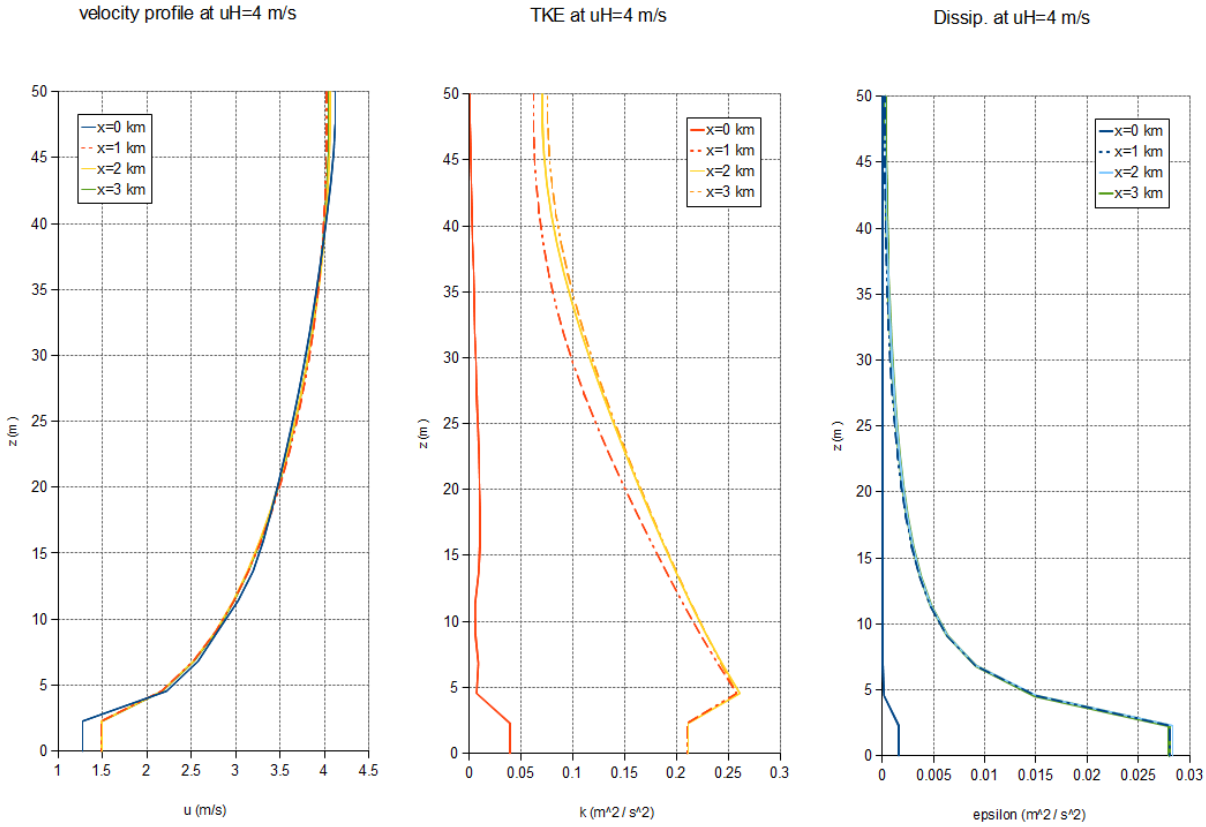

Figure 17. Vertical profile for flow speed, turbulent kinetic energy (TKE) and turbulent dissipation for uH=4 m/s.

5.3 Analysis

5.3.1 Modelled data

From Figure 11 we can see that the time-averaged horizontal velocity profiles for $u_H = \{1,2,...4\,\text{m/s}\}$ and all heights above the seabed have stabilised to within 1% of their final values. This is also evidenced from the vertical velocity profiles in Figure 14, Figure 15, Figure 16 and Figure 17. The turbulent kinetic horizontal profiles in Figure 12 and the vertical profiles in Figure 14, Figure 15 and Figure 16 show k taking longer to reach stable values, particularly at the surface, defined by z=50m, where the TKE levels are lower, agreeing with the profile values at x=2 km and within 5% of the outlet profile at x=3 km. The turbulent dissipation horizontal and vertical plots also show stabilisation by x=2 km.

5.3.2 Comparison with other models and ADCP

Most current measurements with velocity profile specifications from the Sound of Islay are commercially sensitive and so unavailable within the scope of PerAWaT . However, a technical report from Strathclyde University [14] produced a colour map of their modelled velocity profile. From this, a velocity profile was deduced and this has produced an extremely good agreement with the Code Saturne tidal channel model, as shown in Figure 18a. There are discrepancies at $z < 5\,\text{m}$, but these are largely down to approaching the limits of the resolution of the finite volume model; the cells are 2.5m vertically.

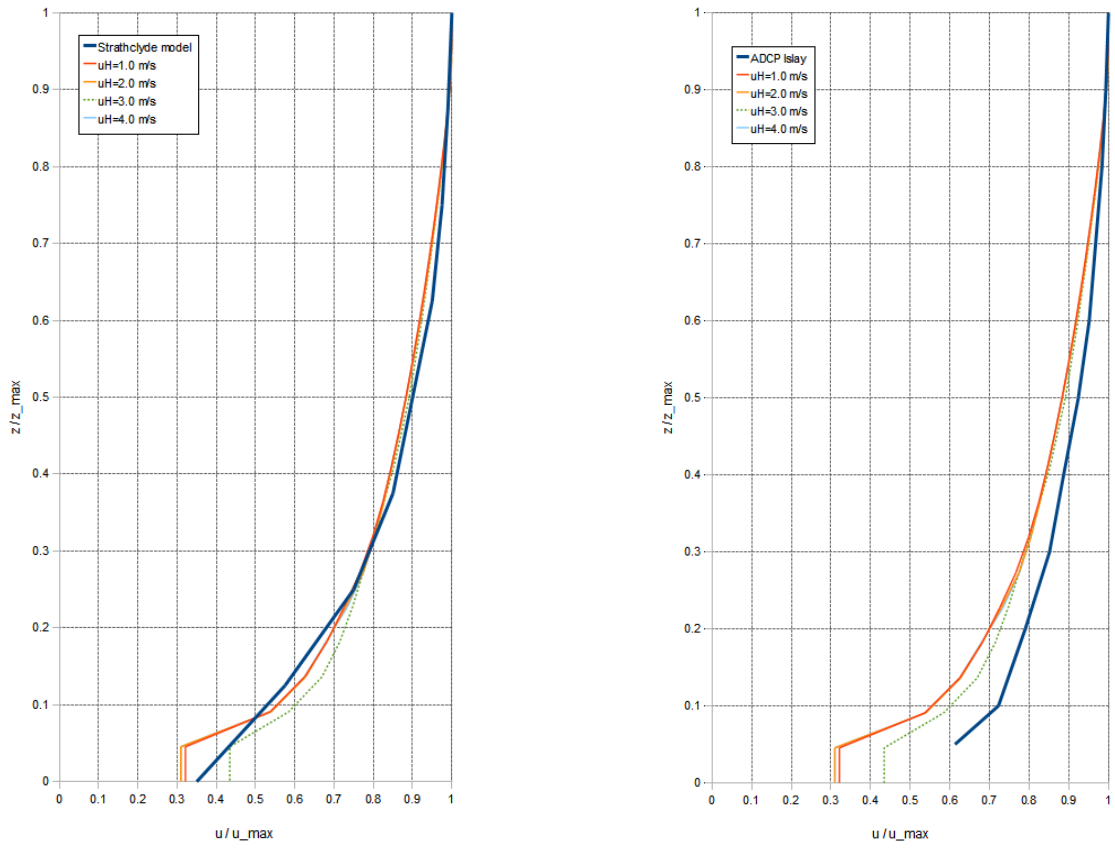

a) b)

Figure 18. Comparison normalised velocity profiles. a) Between Strathclyde's estimated velocity profile for the Sound of Islay [14] and Code Saturne vertical profiles at the channel outlet, for different flow speeds at hub height. b) Between ADCP measurements from the Sound of Islay (courtesy of Iyer [15]) and the Code Saturne model; no ADCP measurements were available for z<2.5m.

A second comparison was made using charts of ADCP measurements from A. Iyer [15] in Figure 18b. Whilst there is agreement at $H = 40\,\text{m}$ ($z/z_{\max} = 0.8$) to within 2% between the ADCP and model profiles, closer to the seabed at $H = 10\,\text{m}$ ($z/z_{\max} = 0.2$), the measured flow speed is 9% smaller. Nonetheless, in the upper middle region where $0.4 < z/z_{\max} < 0.8$ and tidal rotor blades are most likely to be deployed, the flow speeds deviate by a maximum of 4% as shown in Figure 18b. In these tidal cycle simulations, this means an under-prediction of the order of 10^{-1} m/s .

There are perhaps several reasons why the modelled and ADCP velocity profiles differ. Firstly, the bottom of the real Sound of Islay is not flat or straight; it is quite possibly that the undulating channel bed causes local fluctuations in flow and bathymetry, eg. acceleration by narrowing. Secondly, the estimation of the bottom roughness height, $z_0 = 0.2\,\text{m}$, may be at odds with the *local* value of z_0 in the real channel: a detailed map of roughness heights is not readily available. Finally, it is possible that the slightly shallower velocity gradient of the model is due to excess diffusion between higher and lower sections of the fluid. The $k-\varepsilon$ turbulence model uses an isotropic description of turbulence, and oceanic turbulence is highly anisotropic.

6. Summary

The work in D4 is intended to provide a framework for the tidal farm simulations carried out in WG3 WP2 D5b. By using the altered XML configuration file to the default Code Saturne via the GUI, detailed in section 3.2, and use of the **`usclim.F90`** file developed for these simulations, reasonable flow conditions can be provided which are suitable for tidal farm modelling. From the results in section 5, we can see that under a range of tidal flow conditions, the profiles for velocity, turbulent kinetic energy, and turbulent dissipation are guaranteed to be stable for $x \geq 2\,\text{km}$, so $0\,\text{km} < x < 2\,\text{km}$ is defined as the *entry length* in which the flow is still evolving from the boundary conditions, and in which the turbines should not be placed. Placing them beyond the entry length means that the modelled turbine rotors would be exposed to realistic flow conditions.

Small discrepancies were found between ADCP data from the Sound of Islay and the model results, as discussed in section 5.3.2. Unsteady models capable of anisotropic turbulence, such as large eddy simulation (LES), have lent greater accuracy to simulation of such flows in tidal turbine [5], wind turbine and wind farm modelling [16][17][18] However, there is a correspondent additional computational cost. Unsteady RANS using $k-\varepsilon$ has the virtue of being relatively cheap to run – Churchfield's paper [18] details LES simulations running across 4096 processors – and given its known short-comings, has been shown to perform reasonably well.

In conclusion, having been developed and validated, the methodology in this work package can now be directly applied with confidence to WG3 WP2 D5b, where a tidal turbine farm will be simulated in an idealised tidal channel.

7. References

[1] Scottish Power Renewables. *Sound of Islay Demonstration Tidal Array – Non-technical Summary*. Report, July 2010.

[2] C. Geuzaine and J.-F. Remacle. Gmsh: a three-dimensional finite element mesh generator with built-in pre- and post-processing facilities. *International Journal for Numerical Methods in Engineering*, Volume 79:1309-1331, 2009.

[3] J. Uribe. Discretision in Code_Saturne. Technical training manual. *University of Manchester*, 2011 (available online).

[4] EDF R&D Single Phase Thermal-Hydraulics Group. Code_Saturne version 2.1.1 practical user's guide. Technical manual. *EDF*, 2011.

[5] A.C.W. Creech. A three-dimensional numerical model of a horizontal axis, energy extracting turbine. PhD thesis. *Heriot-Watt University*, 2009.

[6] Z-J. You. Estimation of mean seabed roughness in a tidal channel with extended log-fit method. *Continental Shelf Research*, 26:283-294, 2006.

[7] R.G. Lueck and Y. Lu. The logarithmic layer in a tidal channel. *Continental Shelf Research*, 17:1785-1801, 1997.

[8] K. Yamaguchi et al. A continuous mapping of tidal current structures in the Kanmon Strait. *Journal of Oceanography*, 61:283-294, 2005.

[9] M.Q. Nguyen. *K-omega SST not applicable for roughness study in Saturne*. Code Saturne online forums (http://code-saturne.org/forum/viewtopic.php?f=9&t=842). Last accessed 6th Sept 2012.

[10] D.C. Wilcox. Turbulence modelling for CFD (3rd ed.). D C W Industries, 2006.

[11] I.A. Milne et al. Characteristics of the onset flow turbulence at a tidal-stream power site. *Proceedings of the 9th European Wave and Tidal Energy Conference*, Southampton, 2011.

[12] E. Osalusi. Analysis of wave and current data in a tidal energy test site. PhD thesis. *Heriot-Watt University*, 2010.

[13] Ye Li et al. Inflow measurement in a tidal strait for deploying tidal current turbines – lessons, opportunities and challenges. *Proceedings of the ASME 29th conference on Ocean, Offshore and Arctic Engineering*, 2010.

[14] J. Glynn, K. Hamilton, M. MacDonald and T. McCombes. *Tidal current resource and technology methodology*. Technical report / presentation. Strathclyde University, 2012. Available online at http://www.esru.strath.ac.uk/EandE/Web_sites/05-06/marine_renewables/Team/assets/FINAL%20CRIT.ppt

[15] A. Sankaran Iyer. *New methodologies and scenarios for evaluating tidal current energy potential*. PhD Thesis. University of Edinburgh, 2011.

[16] A.C.W. Creech, W.-G. Früh, and P. Clive. Actuator volumes and hr-adaptive methods for 3D simulation of wind turbine wakes and performance. *Wind Energy*, 2011.

[17] M. Germano, U. Piomelli, P. Moin and W.H. Cabot. A Dynamic Subgrid-Scale Eddy Viscosity Model. *Proceedings of Summer Workshop*, Center of Turbulence Research, Stanford University, 1990.

[18] M.J. Churchfield, S. Lee, P.J. Moriarty, L.A. Martínez, S. Leonardi, G. Vijayakumar and J.G. Brasseur. A Large-Eddy Simulation of Wind-Plant Aerodynamics. *50th AIAA Aerospace Sciences Meeting including the New Horizons Forum and Aerospace Exposition*, 2012.